

COMPARISON OF ELECTRO-THERMAL PERFORMANCE OF HETEROJUNCTION BIPOLAR TRANSISTORS BASED ON Si/SiGe AND AlGaAs/GaAs

Roberto Marani & Anna Gina Perri*

Electrical and Electronic Department, Polytechnic University of Bari, Italy

*Phone: +39-80-5963314/5963427; *Fax: +39-80-5963410; *E-mail: perri@poliba.it

ABSTRACT

The aim of this paper is to present a comparison of electro-thermal performance of two HBTs based on Si/SiGe and on AlGaAs/GaAs, by means of an analytical electro-thermal model, already proposed by us, able to calculate the temperature and current distribution for any integrated device, whose structure can be represented as an arbitrary number of superimposed layers with a 2-D embedded thermal source.

Keywords: *Heterojunction Bipolar Transistors, Modelling, SiGe, GaAs, Electrothermal Effects, Self Heating Modelling, RF Devices*

1. INTRODUCTION

One of the main differences between Si based VLSI and RF electronics is the choice of semiconductor materials and transistor types. While Si is the only semiconductor used in VLSI, a wide range of alternative materials and devices are present in RF electronics.

Heterojunction bipolar transistors (HBTs) have attained enough maturity as RF power devices due to their intrinsic high-power density, linearity and efficiency [1]. Moreover HBTs are actually used in very high speed applications. They are capable of microwave performance up to 10 GHz. In order to push the frequency performance up to its limit, the operating point of the HBT lies at relatively high current density, and this current density increases with used semiconductor technologies. Therefore it is important to study the electro-thermal performance, because the self heating appears, mainly in the base-collector depletion region, where both current and field are high.

In this paper we present a comparison of electro-thermal performance of two HBTs based on Si/SiGe and on AlGaAs/GaAs, by means of an analytical electro-thermal model, already proposed by us [2-5]. In particular the problem of the self-heating of transistors fabricated on GaAs substrates has been investigated since GaAs has a poor thermal conductivity. Two problems arise as a consequence: firstly the electrical operating point is directly related to the thermal design giving a significant change in the frequency response of the device; secondly, the chip reliability could be lowered by the temperature increase causing catastrophic damage or gradual performance degradation.

The presentation of the paper is organized as follows. In Section 2 the state-of-the-art of thermal models is briefly summarised, while in Section 3 a short description of the our electro-thermal model is described. The results and relative discussion are given in section 4. The conclusions are described in Section 5.

2. STATE-OF-THE-ART OF THERMAL MODELS

A first classification of thermal models is based on the method used to solve the time-dependent heat equation for transient analysis:

$$-\rho c \frac{\partial T(x, y, z, t)}{\partial t} + \nabla \cdot [k_{TH}(T) \nabla T(x, y, z, t)] = -Q(x, y, z, T, t) \quad (1)$$

or the steady-state heat equation:

$$\nabla \cdot [k_{TH}(T) \nabla T(x, y, z)] = -Q(x, y, z, T) \quad (2)$$

where t is the time, $k_{TH}(T)$ is the temperature-dependent thermal conductivity, c is the specific heat, ρ is the density of the material, $T(x, y, z, t)$ is the temperature field and $Q(x, y, z, T, t)$ is the dissipated power density, which is both temperature and time dependent.

There are two basic approaches to solve both (1) and (2), i.e. the numerical and the analytical technique. The solution of (1) involves the Laplace transform in the analytical case or time-windowing techniques, which are very time-consuming, in the numerical case. In the microwave frequency range the thermal phenomena are much slower than the electrical parameter changes and so this paper addresses the solution of (2) in the steady-state condition.

Numerical solvers of (2), based on the finite-element (FEM) [6], finite-difference (FDM) [7], transmission line matrix (TLM) [8] or boundary-element method (BEM) [9] have been proposed, but all of them are characterised by long numerical calculations.

Many authors have solved either (1) or (2) analytically and interesting solutions were obtained both with the method of separating variables in Cartesian or cylindrical coordinates [10] [11] and the Fourier transform of the thermal field [12]. In the former case the sum of infinite harmonic terms has to be truncated to be able to carry out the calculation without loss in accuracy or taking a long computational time, depending on the number of terms to include. In the latter case the 2-D back transformation is particularly critical.

One difficulty is to handle the non-linear nature of (2) where both k_{TH} and Q are temperature-dependent. Joyce [13] introduced the Kirchhoff transform:

$$\Delta\theta(x, y, z) = \frac{1}{k_0} \int_{T_0}^{T(x,y,z)-T_0} k(\tau) d\tau \quad (3)$$

so as to linearise (2):

$$\nabla^2\theta(x, y, z) = \frac{-Q(x, y, z)}{k_0} \quad (4)$$

where $\Delta\theta(x,y,z)=\theta(x,y,z)-T_0$, $\theta(x,y,z)$ is the transformed temperature field, T_0 is the reference temperature and k_0 is the constant thermal conductivity, evaluated at a specific reference temperature T_0 . In this way the solution of the transformed problem with the unknown $\Delta\theta$ is equivalent to the solution of the original non-linear problem with the unknown ΔT , when the inverse transform is carried out [14].

Another classification is based on the level of coupling between electrical and thermal equations. A fully self-consistent electro-thermal model was presented in [15], and a full 3-D hydrodynamic model was presented in [16]. However most simulators in literature do not take into account the feedback between current and heat generation. An example of feedback based on a weak electro-thermal coupling was presented in [17] but, in this case, the main drawback was the empirical model of the temperature dependence of the drain current which does not allow the designer to understand the relation among a number of physical parameters such as geometrical lengths involved in the layout, thermal resistance, average and peak temperature.

Most of the general purpose commercial thermal simulators can perform the calculations for electronic components and packaging using finite-element techniques or lumped parameters representing an equivalent static or dynamic electric network. The main drawback of this kind of software is its generality that, for example in the specific case of the analysis of heterojunction transistors, does not allow the comprehension and accountability of the phenomena involved from both a thermal and electrical point of view.

3. BRIEF REVIEW OF OUR ELECTRO-THERMAL MODEL

The thermal model already presented by us [2-5] is able to calculate the temperature and current distribution for any integrated device, whose structure, shown in Fig. 1, can be represented as an arbitrary number of superimposed m layers with a 2-D embedded thermal source, so as to include the effect of the package.

For a complete model, the contribution of the mounting and die-attachment layers (see layers (c) and (d) in Fig. 1) to the temperature rise and thermal resistance has been taken into account. The top path for the heat flux has also been included, e.g. mould compound (see layer (g)), where natural convection between the package top surface and the still air is the mechanism of heat loss.

The steady-state problem (2), with temperature-dependent thermal conductivity, is transformed to the simpler linear problem (4) by the use of the Kirchhoff transform (3), by assuming $k_{TH}(T) = k_{TH}(T_0) = k_0$. In this way the transformed problem defined by the well-known Poisson equation is solved and the actual solution of (2) is obtained by the inverse transformation. In the model the heat source is split into a number of elementary point sources. The linearity, and consequently the superposition of the thermal effects due to the elements, is not applied to (2) but to (4), which is mathematically correct. The overall solution of (4) is back-transformed to obtain the thermal field of the non-linear problem described by (2).

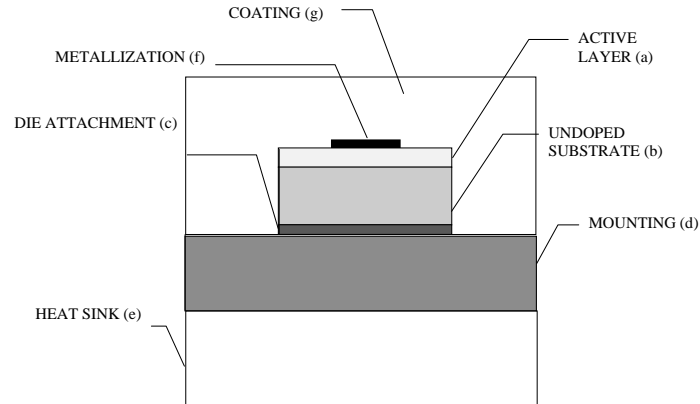


Figure 1. Typical electron device including coating, die attachment, mounting and heat sink.

The electro-thermal feedback is considered by evaluating the output current as a function of the local temperature in the active region and iterating the solution of (4) using the actual value of $Q(\theta)$, as explained in the following subsection.

3.1 Electro-thermal model applied to HBT

In order to solve (4), we are referred to a typical HBT structure [1], in which we have used the name AlGaAs/GaAs HBT for a device with GaAs as the base material and AlGaAs as the emitter. This is also the same for SiGe based transistors.

In particular we have represented the device as a surface without any thickness, where X and Y are the dimensions of the periodic cell, in which we have divided the device.

The overall heat source, which is located in the depletion layer at the collector, has been divided into a set of elementary point sources located in the middle of each elementary $X \times Y$ periodic cell.

The first step is to solve the electro-thermal problem, assuming the heat generation and the current as mutually dependent for each single elementary device which is related to a single elementary heat source; finally the resulting thermal field of the whole structure is obtained by the superposition of all the elementary fields.

The solution of (4) for a point thermal source can be expressed as [18]:

$$\Delta\theta(x, y, z) = \frac{Q(x_{0i}, y_{0i}, z_{0i})}{2\pi\pi_0 \sqrt{(x - x_{0i})^2 + (y - y_{0i})^2 + (z - z_{0i})^2}} \quad (5)$$

where x_{0i} , y_{0i} and z_{0i} are the coordinates of the i -th heat point source, x, y, z is the generic position in which the temperature increase $\Delta\theta(x, y, z)$ above the reference is evaluated and $Q(x_{0i}, y_{0i}, z_{0i})$ is the dissipated power of the i -th elementary heat source.

The electro-thermal feedback can be implemented for each $X \times Y$ subsection considering that Q can be assumed as the temperature-dependent electrical power $P(\theta_i(x_{0i}, y_{0i}, z_{0i}))$ of the i -th elementary device centred in x_{0i} , y_{0i} , z_{0i} and, thus, corresponding to the i -th heat source centred in the same point.

The electrical power of the i -th elementary device is:

$$P(x_{0i}, y_{0i}, z_{0i}) = P(\theta_i) = I_B(\theta_i) V_{BE} + I_C(\theta_i) V_{CE} \quad (6)$$

where V_{BE} , the voltage drop between base and emitter, is temperature-independent, I_B and I_C are the base and collector currents, respectively, of the elementary cell centred in x_{0i}, y_{0i}, z_{0i} having temperature θ_i , and V_{CE} , the voltage drop between collector and emitter, is temperature-independent.

The dependence of the current-voltage equation, based on physical parameters, on the temperature was widely studied in the past. The parameters that have been taken into account for their thermal dependence are the electron mobility, saturation velocity, permittivity, energy band gap, threshold voltage and built-in voltage. The reader can refer to for the empirical expression of the foregoing parameters [18].

4. SIMULATION RESULTS AND DISCUSSION

We have firstly extracted, by a MATLAB code written *ad hoc*, the Si/SiGe and AlGaAs/GaAs HBTs I-V curves versus bias using the Gummel-Poon model, whose parameters are those of SPICE simulator [19-21].

4.1 HBT based on Si/SiGe

We have considered a HBT structure having $X = 0.25 \mu\text{m}$ and $Y = 30 \mu\text{m}$ for the emitter and $X = 50 \mu\text{m}$ and $Y = 300 \mu\text{m}$ for the collector.

In Fig. 2 we have reported the I_C - V_{CE} characteristics at room temperature $T = 300 \text{ K}$, for a base current varying from 1 mA to 3 mA..

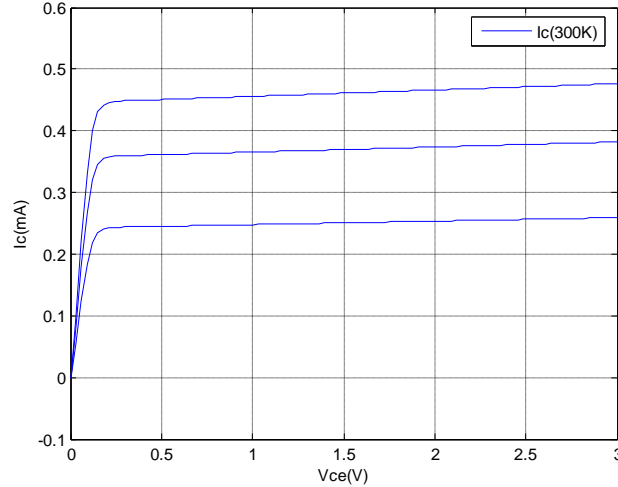


Figure 2. Simulated I_C - V_{CE} characteristics at $T=300 \text{ K}$ for a base current varying from 1 mA to 3 mA.

The obtained heat generated at the base-collector junction, by Eq. (6), has been equal to 0.0702 W.

Now it has been possible determined the temperature increase due to self heating effect.

Fig. 3 shows the simulated average temperature T_m at the BE junction versus time, in the time range $10^{-8} \div 10^{-3} \text{ s}$.

In the interval $10^{-6} \div 10^{-5} \text{ s}$, it clearly appears that the temperature increases more rapidly, tending to a saturation value equal to 7.85 K.

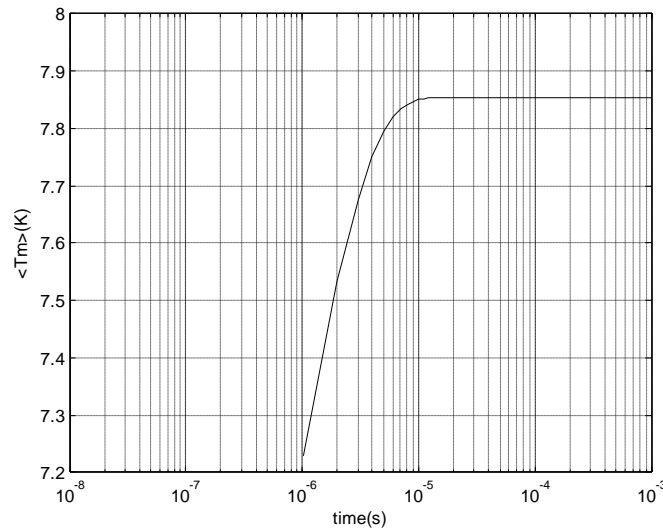


Figure 3. Simulated average temperature T_m at BE junction versus time for Si/SiGe HBT.

The electro-thermal feedback is shown in Fig. 4, in which we have reported the simulated output I-V characteristics both at 300 K (blue lines) and at 307.85 K (red lines). This figure shows the well-known degradation effect on I-V curves due to temperature increase.

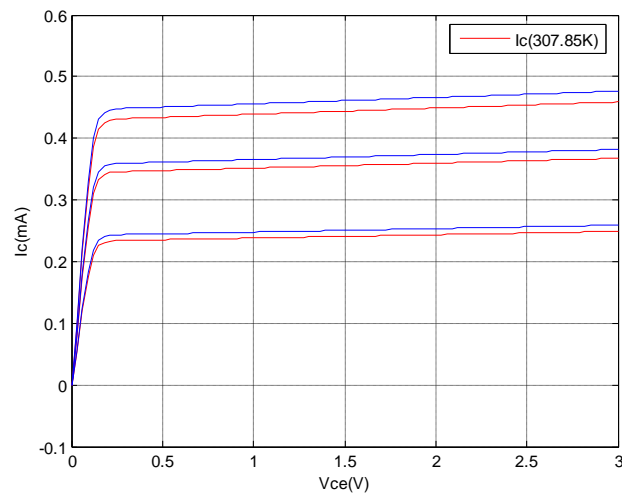


Figure 4. Simulated I-V characteristics both at 300 K (blue lines) and at 307.85 K (red lines).

We have considered a Si/SiGe HBT, whose structure is the same of the previous one, except for the dimension X of the emitter, equal, in this case, to $2.5 \mu\text{m}$.

Fig. 5 shows the simulated average temperature T_m at the BE junction versus time. For this device the saturation value of T_m is 4.55 K and this result allows to say that the self heating is in inverse proportion to the emitter area. Moreover, as shown in Fig. 6, in which we have reported the simulated I-V curves both at 300 K (blue lines) and at 304.55 K (red lines), the device feels more the effects of temperature increase at high base currents, with a resulting decrease of device efficiency.

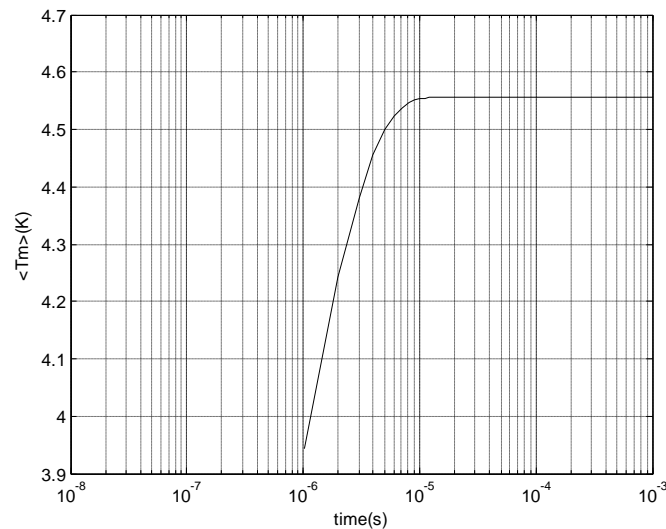


Figure 5. Simulated average temperature T_m at BE junction versus time ($X=2.5 \mu\text{m}$ for the emitter).

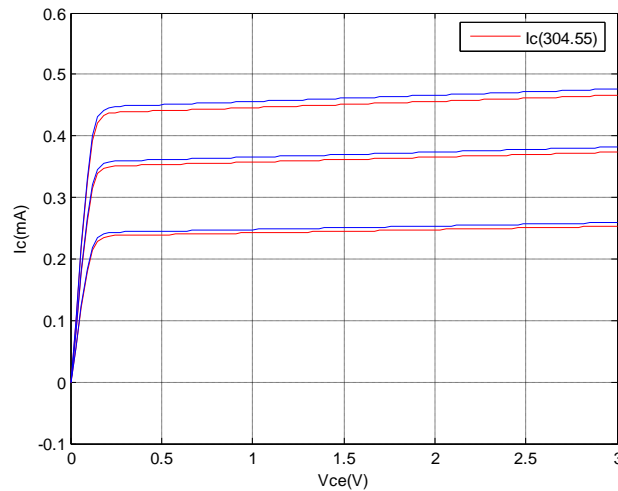


Figure 6. Simulated I-V characteristics both at 300 K (blue lines) and at 304.55 K (red lines).

4.2 HBT based on AlGaAs/GaAs

We have repeated the same simulations, considering now an AlGaAs/GaAs HBT, having $X = 0.25 \mu\text{m}$ and $Y = 30 \mu\text{m}$ for the emitter and $X = 50 \mu\text{m}$ and $Y = 300 \mu\text{m}$ for the collector.

In Fig. 7 we have reported the I_C - V_{CE} characteristics at room temperature $T = 300 \text{ K}$, for a base current varying from 1 mA to 3 mA.. The obtained heat generated at the base-collector junction, calculated by Eq. (6), has been, for this device, equal to 0.0508 W.

The temperature T_m versus time is shown in Fig. 8, in which it clearly appears that T_m tends to a saturation value equal to 8.4 K.

The electro-thermal feedback is shown in Fig. 9, in which we have reported the simulated output I-V characteristics both at 300 K (blue lines) and at 308.4 K (red lines).

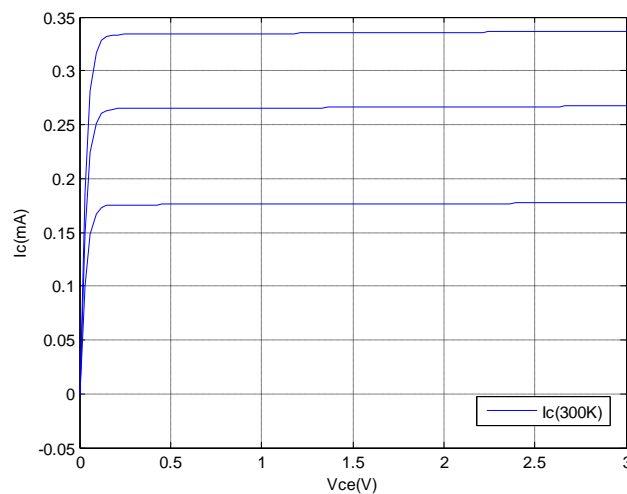


Figure 7. Simulated I_C - V_{CE} characteristics at $T=300 \text{ K}$ for a HBT based on AlGaAs/GaAs

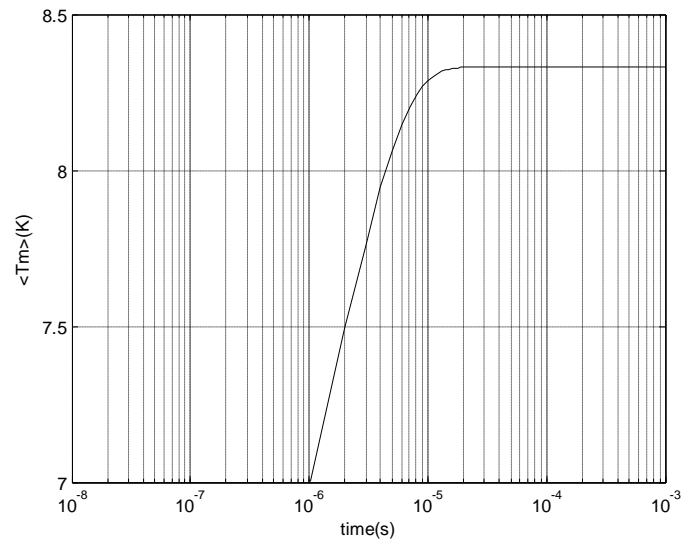


Figure 8. T_m at BE junction versus time for AlGaAs/GaAs HBT.

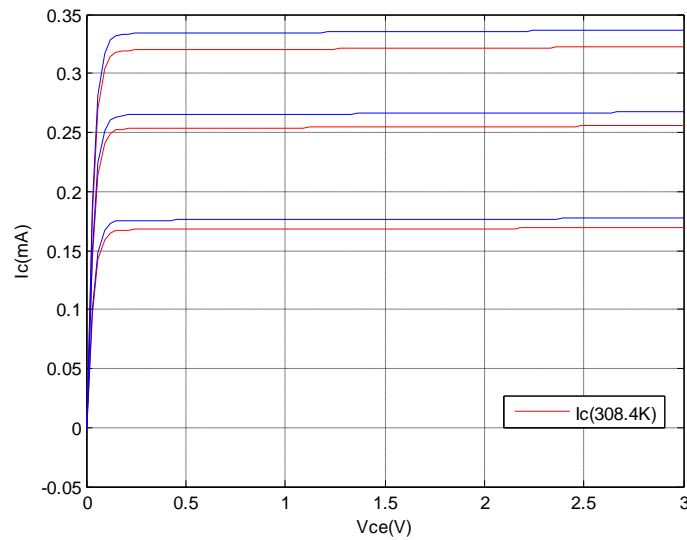


Figure 9. Simulated I-V characteristics both at 300 K (blue lines) and at 308.4 K (red lines).

Also for this device, we have modified the emitter dimension ($X = 2.5 \mu\text{m}$), obtaining that the saturation value of T_m becomes 5.4 K, as shown in Fig. 10.

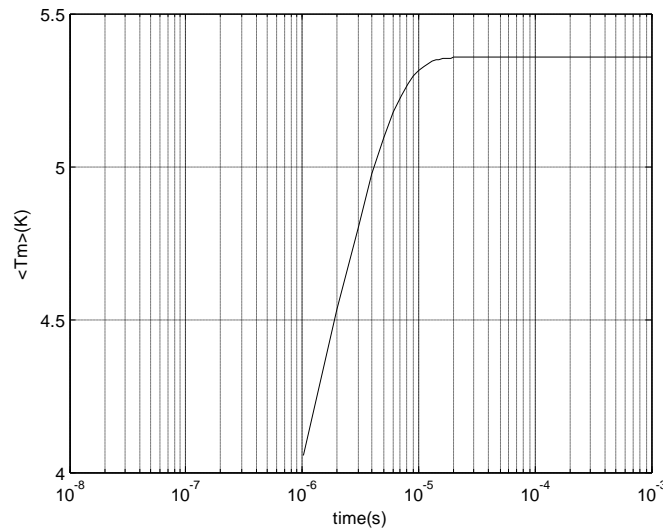


Figure 10. T_m at BE junction versus time for AlGaAs/GaAs HBT ($X=2.5 \mu\text{m}$ for the emitter).

At last, in Fig. 11 we have reported the temperature T_m versus time for two HBTs having the same dimensions, but different substrates (Si, red line and GaAs, blue line). It is easy to observe that Si substrate allows to have smaller values of T_m , with a transitory time shorter.

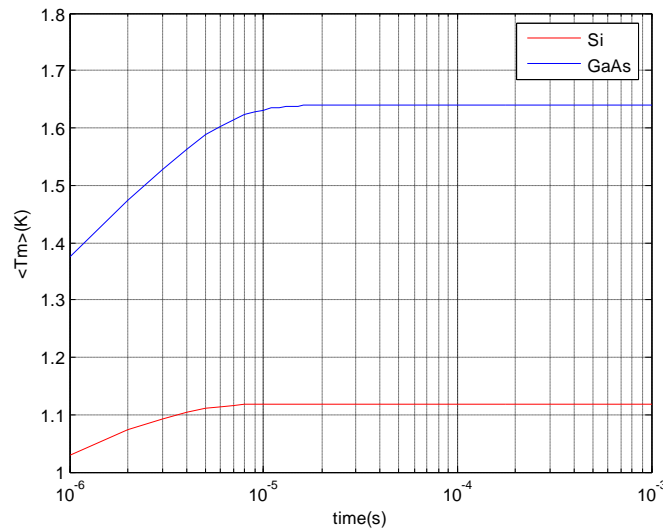


Figure 11. T_m versus time for two HBTs having different substrates (Si, red line and GaAs, blue line).

Finally, considering the Early effect, the breakdown voltage values in Si/SiGe HBT are relatively low due to their smaller band-gap of the collector material. This makes it more difficult to use them for high-power applications [21] [22], where AlGaAs/GaAs HBTs are preferred. However, this problem can be reduced by the DHBT approach since designing the collector–base junction as a heterojunction allows to use a wide band-gap material as the collector material leading to high-breakdown values.

5. CONCLUSIONS

In this paper we have presented a comparison of electro-thermal performance of two HBTs based on Si/SiGe and on AlGaAs/GaAs, by means of an analytical electro-thermal model, already proposed by us, able to calculate the temperature and current distribution for any integrated device, whose structure can be represented as an arbitrary number of superimposed layers with a 2-D embedded thermal source. In particular the problem of the self-heating of transistors fabricated on GaAs substrates has been investigated since GaAs has a poor thermal conductivity.

The electro-thermal feedback is considered by evaluating the output current as a function of the local temperature in the active region.

Moreover it has been possible determined the temperature increase due to self heating effect, in order to evaluate the average temperature T_m at the BE junction. In this way we have demonstrated that Si substrate allows to have smaller values of T_m , with a transitory time shorter.

6. REFERENCES

- [1]. A. G. Perri: Dispositivi Elettronici Avanzati, Progedit Editor, Bari, Italy; ISBN: 978-88-6194-081-9, (2011).
- [2]. R. Marani, A.G. Perri: Thermal and Electrical Layout Optimisation of Multilayer Structure Solid-State Devices based on the 2-D Fourier series, *Proceedings of MELECON 2010*, Valletta, Malta, (2010).
- [3]. R. Marani, A.G. Perri: Analytical Electrothermal Modelling of Multilayer Structure Electronic Devices, *The Open Electrical & Electronic Engineering Journal*, ISSN:1874-1290, **4**, 32-39, (2010).
- [4]. A. G. Perri: Modelling and Simulations in Electronic and Optoelectronic Engineering, Research Signpost, Kerata, India, 2011, ISBN: 978-81-308-0450-7, (2011).
- [5]. A.G. Perri, R. Marani: Electrothermal Design of Multilayer Structure Integrated Devices through the Solution to the non-linear 3-D Heat Flow Equation, in *Modelling and Simulations in Electronic and Optoelectronic Engineering*, Research Signpost, Kerata, India, ISBN 978-81-308-0450-7, 1-26, (2011).
- [6]. L. M. Mahalingham, J. A. Andrews, J. E. Drye: Thermal studies on pin grid array packages for high density LSI and VLSI logic circuits, *IEEE Transactions on Components Packaging and Manufacturing Technology*, **6**, 246-256, (1983).
- [7]. P. W. Webb: Thermal modeling of power GaAs microwave integrated circuits, *IEEE Transactions on Electron Devices*, **40**, 867-877, (1993).
- [8]. C. C. Lee, A. L. Palisoc, J. M. W. Baynham: Thermal analysis of solid state devices using the boundary element method, *IEEE Transactions on Electron Devices*, **35**, 1151-1153, (1988).
- [9]. P. W. Webb, A. D. Russell: Application of the TLM method to transient thermal simulation of microwave power transistor, *IEEE Transactions on Electron Devices*, **42**, 624-631, (1995).
- [10]. A. G. Kokkas: Thermal analysis of multiple-layer structures, *IEEE Transactions on Electron Devices*, **21**, 674-681, (1974).
- [11]. P. Hui, H. S. Tan: Temperature distribution in a heat dissipation system using a cylindrical diamond heat spreader on a copper heat sink, *Journal of Applied Physics*, **75**, 748-757, (1994).
- [12]. D. H. Chien, C. Y. Wang, C. C. Lee: Temperature solution of five layer structure with a circular embedded source and its applications, *IEEE Transactions on Components Hybrids and Manufacturing Technology*, **15**, 707-714, (1992).
- [13]. W. B. Joyce: Thermal resistance of heat sinks with temperature-dependent conductivity, *Solid State Electronics*, **18**, 321-322, (1975).
- [14]. D. H. Smith: Predicting operating temperature for GaAs ICs, *GaAs IC Symposium 1991*, 187-190, (1991).
- [15]. V. C. Alwin, D. H. Navon, L. J. Turgeon: Time-dependent carrier flow in a transistor structure under nonisothermal conditions, *IEEE Transactions on Electron Devices*, **24**, 1297-1304, (1977).
- [16]. G. K. Wachutka: Rigorous thermodynamic treatment of heat generation and conduction in semiconductor device modelling, *IEEE Transactions on CAD*, **9**, 1141-1149, (1990).
- [17]. L. Semi, B. Riccò: Modeling temperature effects in the DC I-V characteristics of GaAs MESFETs, *IEEE Transactions on Electron Devices*, **40**, 273-277, (1993).
- [18]. R. Anholt: Electrical and thermal characterization of MESFETs, HEMTs and HBTs, Artech House Inc., ISBN:0-89006-749-X, (1995).
- [19]. <http://hbt.ucsd.edu>.
- [20]. www.ece.usb.edu/Faculty/rodwell/Classes/ECE594A/.
- [21]. O. Esame, Y. Gurbuz, I. Tekin, A. Bozkurt: Performance comparison of state-of-the-art heterojunction bipolar devices (HBT) based on AlGaAs/GaAs, Si/SiGe and InGaAs/InP, *Microelectronics Journal*, **35**, 901-908, (2004).
- [22]. P. Y. Sulima, J. Battaglia, T. Zimmer, J.-C. Batsale: Self heating modeling of SiGe heterojunction bipolar transistor, *International Communications in Heat and Mass Transfer*, **34**, 553-563, (2007).